

Restoring Size Consistency of Approximate Functionals Constructed from the Adiabatic Connection

Stefan Vuckovic,^{*,†} Paola Gori-Giorgi,[†] Fabio Della Sala,[‡] and Eduardo Fabiano[‡]

[†]*Department of Theoretical Chemistry and Amsterdam Center for Multiscale Modeling, FEW, Vrije Universiteit, De Boelelaan 1083, 1081HV Amsterdam, The Netherlands*

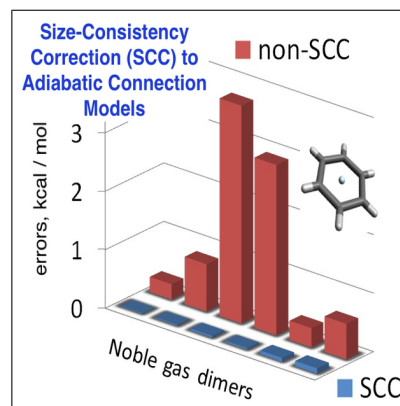
[‡]*Institute for Microelectronics and Microsystems (CNR-IMM), Via Monteroni, Campus Unisalento, 73100 Lecce, Italy*

E-mail: s.vuckovic@vu.nl

Abstract

Approximate exchange-correlation functionals built by modeling in a non-linear way the adiabatic connection (AC) integrand of density functional theory have many attractive features, being virtually parameters-free and satisfying different exact properties, but they also have a fundamental flaw: they violate the size-consistency condition, crucial to evaluate interaction energies of molecular systems. We show that size consistency in the AC-based functionals can be restored in a very simple way at no extra computational cost. Results on a large set of benchmark molecular interaction energies show that functionals based on the interaction strength interpolation approximations are significantly more accurate than the second-order perturbation theory.

Graphical TOC Entry



With applications that stretch from solid state physics to biochemistry, Kohn-Sham density functional theory (KS-DFT)¹ is presently the most employed electronic structure method. Although the theory is in principle exact, any practical implementation of KS-DFT must rely on approximations for the exchange-correlation (XC) functional, which should capture all the many-body effects beyond the simple Hartree theory. Despite the existence of hundreds of different XC approximations^{2,3} and their widespread success in various disciplines,² KS-DFT still encounters open issues, which hamper its overall predictive power^{2,4-6} and make the quest for better approximations a crucial research field for computational chemistry, solid state physics and materials science.^{2,4-6}

The density-fixed adiabatic connection (AC) formalism^{7,8} provides an exact expression for the XC energy functional $E_{xc}[\rho]$,

$$E_{xc}[\rho] = \int_0^1 W_\lambda[\rho] d\lambda, \quad (1)$$

where $W_\lambda[\rho]$ is the AC integrand,

$$W_\lambda[\rho] = \langle \Psi_\lambda[\rho] | \hat{V}_{ee} | \Psi_\lambda[\rho] \rangle - U[\rho], \quad (2)$$

$\Psi_\lambda[\rho]$ is the fermionic wavefunction with density $\rho(\mathbf{r})$ that minimizes the sum of the kinetic energy \hat{T} and of the electron-electron repulsion \hat{V}_{ee} scaled by the coupling constant λ , and $U[\rho]$ is the Hartree energy. For small systems, $W_\lambda[\rho]$ has also been computed exactly through eq 2. However, this requires the solution of the many-body Schrödinger equation.⁹⁻¹¹ Thus, to all practical purposes $W_\lambda[\rho]$ must be approximated.

Equation 1 has been a fundamental milestone in guiding the construction of approximations. Early AC-based XC functionals used forms that depend linearly on some chosen input ingredients, such as the exchange energy from Hartree-Fock theory as value to be recovered at $\lambda = 0$, and semilocal approximations at some $\lambda = \lambda_p$ between 0 and 1. These forms are commonly used for the construction of hybrid¹²⁻¹⁴ and double-hybrid¹⁵⁻¹⁷ density functionals, resulting in mixing a fixed fraction of Hartree-Fock

exchange and second-order perturbation theory with semilocal functionals. They often work well for main-group chemistry, but they show important limitations for various other problems as for example the chemistry of transition metals¹⁸ (where they even worsen the results with respect to simpler semilocal functionals), metal-molecule interfaces,¹⁹ and even non-covalent bonding (unless an ad hoc van der Waals correction is used).^{20,21} Their main disadvantage is that the mixing fractions are fixed and cannot adapt to different systems or to different parts of a system.

To address this problem, several models in which the input ingredients enter in a non-linear way have been proposed.^{11,22-26} These latter forms do not need to rely on empiricism, and can adapt automatically to the peculiarities of the system under study. Along these lines, Ernzerhof had proposed Padé forms for the λ -dependence of the AC integrand,²² which later were used for the construction of the MCY family of functionals that are constrained to be free of one-electron self-interaction error.^{25,27} Another example of models that use input ingredients in a non-linear way is provided by the interaction strength interpolation (ISI) functionals, which depend explicitly on the weak- and strong-coupling ingredients,^{23,24,28-30} essentially extending to non-uniform densities Wigner's^{31,32} idea for approximating the energy of the homogeneous electron gas. Despite the advantages of the nonlinear forms over the linear ones, the former encounter a fundamental flaw: the XC functionals that are constructed from them are not size-consistent for systems composed by different species of fragments.^{27,33} This depends on the fact that these methods employ as input ingredients global quantities (integrated over all space). A route that is currently being explored addresses this issue by modeling the AC at each given spatial position \mathbf{r} , using energy densities $w_\lambda(\mathbf{r})$ ^{26,34-36} instead of quantities integrated over all space. This strategy is very promising, but does not allow using in a straightforward way semilocal ingredients,^{26,33-39} because of the inherent ambiguity in the definition of energy densities, a problem shared with the construction of local hybrid

functionals.^{37,40,41}

In this Letter we show that size consistency of the *global* (integrated over all space) AC forms in which the ingredients enter in a non-linear way can be restored in a remarkably simple way, making it possible to obtain meaningful interaction energies at no additional computational cost.

Consider a system M (e.g., a molecular complex) composed of a set of fragments A_i , with $i = 1, \dots, N$. The interaction energy is a key quantity in chemistry and it is defined as

$$E^{\text{int}}(M) = E(M) - \sum_{i=1}^N E(A_i), \quad (3)$$

where $E(M)$ is the energy of the bound system M and $E(A_i)$ are the energies of the individual fragments. If we now compute the energy of a system M^* made of the same fragments A_i placed at a very large (infinite) distance from each other, any size-consistent method should give $E^{\text{int}}(M^*) = 0$, or equivalently

$$E(M^*) = \sum_{i=1}^N E(A_i). \quad (4)$$

We should stress at this point that size consistency in DFT is in general a very subtle issue, particularly when dealing with fragments with a degenerate ground state (e.g., open-shell atoms), as the (spin) density is not anymore an intensive quantity.^{42,43} To disentangle this more general DFT problem from the one of size-consistency of the non-linear AC models, here we focus on the cases where the fragments have a non-degenerate ground-state,⁴⁴ considering non-covalent interactions.

The idea behind AC-based functionals is to use a certain number of input ingredients $W_i[\rho]$, constructing a λ -dependent function that interpolates between them. For example, many standard hybrid functionals model $W_\lambda[\rho]$ with functions of the kind

$$W_\lambda^{\text{hyb}}[\rho] = W_\lambda^{\text{DFA}}[\rho] + (E_x^{\text{HF}}[\rho] - E_x^{\text{DFA}}[\rho])\lambda^{n-1}, \quad (5)$$

where $W_\lambda^{\text{DFA}}[\rho]$ is a given density-functional approximation (usually a semilocal functional),

with its exchange component $W_{\lambda=0}^{\text{DFA}}[\rho] = E_x^{\text{DFA}}[\rho]$, and $E_x^{\text{HF}}[\rho]$ is the Hartree-Fock (HF) exchange energy.

This kind of expressions, when inserted in eq 1, yields a fixed fraction $1/n$ of HF exchange energy mixed with a semilocal density functional approximation. Because the input ingredients, in this case $W_\lambda^{\text{DFA}}[\rho]$, $E_x^{\text{HF}}[\rho]$, and $E_x^{\text{DFA}}[\rho]$, enter linearly in the model of eq 5, the resulting XC functional automatically satisfies the size-consistency condition of eq 4 if the individual ingredients do.

As examples of approximations in which the ingredients enter in a non-linear way, consider first the Padé([1/1]) form introduced by Ernzerhof,²²

$$W_\lambda^{\text{Pad}}[\rho] = a[\rho] + \frac{b[\rho]\lambda}{1 + c[\rho]\lambda}, \quad (6)$$

with $a[\rho] = W_0[\rho] = E_x^{\text{HF}}[\rho]$, $b[\rho] = W'_0[\rho]$ (which can be obtained from second-order perturbation theory), and $c[\rho] = \lambda_p^{-1} - W'_0[\rho](W_0[\rho] - W_{\lambda_p}^{\text{DFA}}[\rho])^{-1}$, where $W_{\lambda_p}^{\text{DFA}}[\rho]$ could be a semilocal functional at a chosen value λ_p . We see immediately that in this case, even if the input quantities W_0 , W'_0 and W_{λ_p} satisfy the size-consistency condition of eq 4, the resulting XC functional from eq 1 does not, because it is given by a non-linear function f^{Pad} of these ingredients, $E_{xc}^{\text{Pad}} = f^{\text{Pad}}(W_0, W'_0, W_{\lambda_p})$.

Another example is the idea of Seidl and co-workers^{23,24} to build approximate $W_\lambda[\rho]$ by interpolating between its weak- ($\lambda \rightarrow 0$) and strong- ($\lambda \rightarrow \infty$) coupling expansions,

$$W_{\lambda \rightarrow 0}[\rho] = W_0[\rho] + \lambda W'_0[\rho] + \dots \quad (7)$$

$$W_{\lambda \rightarrow \infty}[\rho] = W_\infty[\rho] + \frac{W'_\infty[\rho]}{\sqrt{\lambda}} + \dots, \quad (8)$$

which allows avoiding bias towards the weakly correlated regime, and to include more pieces of exact information. The $\lambda \rightarrow 0$ limit of eq 7 is provided by the exact exchange and the second-order perturbation theory, while the functionals $W_\infty[\rho]$ and $W'_\infty[\rho]$ describe a floating Wigner crystal with a metric dictated by the density.^{28,45}

Different formulas that interpolate between the limits of eqs 7 and 8 are available in the literature^{23,24,26,28,46}. As in the Padé example of eq 6, when these interpolation formulas are inserted in eq 1 they give an XC energy that is a nonlinear function of the 4 ingredients (or a subset thereof) $W_0[\rho], W'_0[\rho], W'_\infty[\rho], W_\infty[\rho]$ appearing in eqs 7-8.

It is clear from these examples that we can write a general XC functional obtained by modeling the adiabatic connection as

$$E_{xc}^{\text{ACM}}[\rho] = f^{\text{ACM}}(\mathbf{W}[\rho]), \quad (9)$$

where f^{ACM} is a non-linear function that results from the integration [via eq1] of the given adiabatic connection model (ACM), and $\mathbf{W}[\rho] = \{W_1[\rho], \dots, W_k[\rho]\}$ is a compact notation for the k input ingredients that have been used. Then we have

$$\sum_{i=1}^N E_{xc}^{\text{ACM}}(A_i) = \sum_{i=1}^N f^{\text{ACM}}(\mathbf{W}(A_i)), \quad (10)$$

and

$$E_{xc}^{\text{ACM}}(M^*) = f^{\text{ACM}}\left(\sum_{i=1}^N \mathbf{W}(A_i)\right). \quad (11)$$

This equation is one of the main points in this work. Although conceptually simple, it shows that the energy of a set of infinitely distant fragments (M^*) can be expressed as a function of the quantities of the isolated fragments. Notice that this holds in this special case because f^{ACM} is a function of global size-consistent⁴⁴ quantities. For size-inconsistent wavefunction methods, such as CISD, this is usually not true, and the energy of M^* needs to be computed by performing an extra calculation with the fragments at a large distance, which might be tricky to do in practice.

Essentially all the models that have been proposed in the literature²⁷ satisfy the condition

$$f^{\text{ACM}}(N\mathbf{W}(A)) = Nf^{\text{ACM}}(\mathbf{W}(A)), \quad (12)$$

meaning that they are size-consistent when a system dissociates into equal fragments (size-extensivity). This is also a key difference with

the size-consistency problem of wavefunction methods, which also arises in the case of equal fragments. However, when the A_i are of different species, eqs 10 and 11 give in general different results, and attempts to make them equal for a non-linear model have failed so far.²⁷

As said, evaluating eq 10 or eq 11 has exactly the same computational cost, as both equations only need the input ingredients for the individual fragments. The idea behind the size-consistency correction (SCC) is thus extremely simple and it is related to discussions reported in Refs.:⁴⁷⁻⁴⁹ it consists in using the difference between eq 11 and eq 10 to cancel the size-consistency error that is made when evaluating interaction energies from eq 3,

$$\Delta_{\text{SCC}} = \sum_{i=1}^N f^{\text{ACM}}(\mathbf{W}(A_i)) - f^{\text{ACM}}\left(\sum_{i=1}^N \mathbf{W}(A_i)\right). \quad (13)$$

Note that this correction is fundamentally different from a direct calculation of $\sum_i E(A_i) - E(M^*)$, since, due to the use of eq (11), only the knowledge of the isolated fragments is required here, while there is no need to deal with the (possibly tricky) calculation of the supramolecular energy M^* .

Adding Δ_{SCC} to an interaction energy computed via eq 3 is equivalent to always evaluating interaction energies with respect to eq 11 instead of eq 10, i.e.,

$$E_{xc,\text{int}}^{\text{ACM,SCC}}[\rho] = f^{\text{ACM}}(\mathbf{W}(M)) - f^{\text{ACM}}\left(\sum_{i=1}^N \mathbf{W}(A_i)\right). \quad (14)$$

As an example of the performance of the SCC, we examine here ACMs that link the two limits of eqs 7 and 8. As said, we focus on non-covalent interactions because the fragments A_i have a non-degenerate ground state, which should guarantee size-consistency of the input ingredients.^{42,43} Moreover, in this case the interaction energy is small and so the correction can be relevant: for covalent interactions, in fact, the correction is of the same order of magnitude as for non-covalent ones,

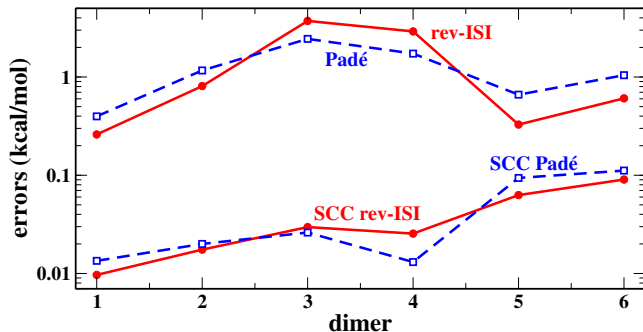


Figure 1: The absolute errors on the interaction energy (kcal/mol, log-scale) for a set of dispersion heterodimers, containing the noble gas atoms, obtained with the rev-ISI and Padé([1/1]) functionals with and without the inclusion of the SCC of eq 13 (1: He-Ne, 2: He-Ar, 3: Ne-Ar, 4: Ar-Kr, 5: CH₄-Ne, 6: C₆H₆-Ne).

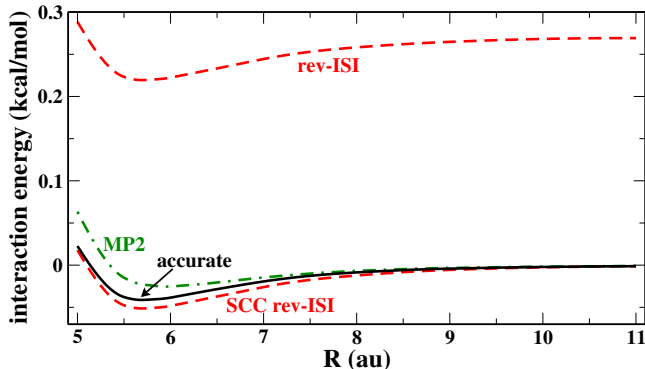


Figure 2: Interaction energy curve for the HeNe heterodimer obtained with the rev-ISI functional with and without the SCC of eq 13. The MP2 curve is shown for comparison and the accurate curve has been taken from Ref. ⁵⁰

but the interaction energy is at least two orders of magnitude larger. All calculations have been performed using a development version of the TURBOMOLE package,^{51,52} with computational details similar to those of Refs. 48 and,⁵³ in which the ISI-like functionals are evaluated on Hartree-Fock orbitals (see Section IV.D of Ref. 53 for some discussion of this choice). Thus, in eq 7 $W_0[\rho] = E_x^{\text{HF}}[\rho]$ and $W'_0[\rho]$ is twice the second-order Möller-Plesset (MP2) correlation energy, $W'_0[\rho] = 2E_c^{\text{MP2}}$. The strong-coupling functionals $W_\infty[\rho]$ and $W'_\infty[\rho]$ of eq 8 are approximated with the point-charge-plus-continuum (PC) semilocal model,⁵⁴ which is reasonably accurate.^{28,45} We test different interpolation formulas that have been proposed in the literature, namely SPL,²³ rev-ISI²⁸ and LB⁴⁶. Additionally, we also tested the Padé[1,1] formula of eq 6 by using $\lambda_p = \infty$. The interpolation formulas and additional computational details are reported in the Supporting Information.

As a first example, in Fig. 1 we show the absolute errors in the interaction energy for a set of dispersion complexes made of fragments of different species obtained from the rev-ISI and the Padé interpolation formulas, computed with and without the SCC. From this figure we can see that in both cases the error is reduced by an order of magnitude when the correction is applied, i.e. when eq 14 is used.

In Figure 2 we also report the interaction energy curve for He-Ne obtained from the rev-ISI functional. We see that the rev-ISI curve has a very reasonable shape, but, because of the size-consistency error, when computed with eq 3 it goes to a positive value with respect to the sum of the fragment energies. Instead, when the SCC is applied, the correct asymptotic value of the dissociation curve (given by eq 11) is used to compute interaction energies. Very similar figures are obtained when we consider other interpolation formulas and other systems, with the overall shift that is sometimes positive and sometimes negative.

Finally, we use the SCC to assess the accuracy of AC-based functionals for more non-covalent complexes relevant for chemistry and biology. For this purpose, we employ the well established

quantum-chemical dataset for non-covalent interactions S66.⁵⁵

In Figure 3 we report the values of

$$\delta_i^{\text{SCC}} = \left| \frac{E_i^{\text{rev-ISI-SCC}} - E_i^{\text{ref}}}{E_i^{\text{ref}}} \right| - \left| \frac{E_i^{\text{rev-ISI}} - E_i^{\text{ref}}}{E_i^{\text{ref}}} \right|, \quad (15)$$

where the index $i = 1, \dots, 66$ labels the various complexes, E_i^{ref} is the reference interaction energy of the i -th complex and $E_i^{\text{rev-ISI-SCC}}$ and $E_i^{\text{rev-ISI}}$ are the corresponding interaction energies calculated with rev-ISI with and without the SCC correction, respectively. Thus a negative (positive) δ_i^{SCC} means that the SCC reduces (increases) the relative error of the interaction energies. Notice that in Figure 3 the S66 complexes are sorted in ascending order according to the computed $|\Delta_{\text{SCC}}|$ value (see inset of Figure 3). Thus, one can see that, for systems where $|\Delta_{\text{SCC}}|$ is non-negligible (i.e. $i \gtrsim 30$), the inclusion of the SCC brings an improvement of the results ($\delta_i^{\text{SCC}} < 0$) and that the improvement can be as large as 10%. On the other hand, there are some systems (i.e. $i \lesssim 30$) with a negligible SCC. This is not surprising, as the S66 dataset contains 17 homodimers, for which the AC-based functionals are already size consistent. Moreover, there is another case in which the size-consistency error becomes negligible: when the ratio $q_i = W_i(A)/W_i(B)$ between the i^{th} input ingredient of fragment A and of fragment B is roughly the same for all i , $q_i \approx q$, a case that becomes mathematically equivalent to eq 12. In summary, Figure 3 shows that the larger is the Δ_{SCC} value, the larger is the reduction of the errors. This indicates that the inclusion of Δ_{SCC} is significant and works correctly for most non-covalent complexes having different constituting units.

More generally, for all the SCC-ISI-like functionals that we examined, the performance for non-covalent interactions is quite good, being comparable or better than state-of-the-art computational approaches (see Table 1). Especially for dispersion and mixed complexes, all the ACMs perform 7 or 8 times better than the B2PLYP double hybrid and twice as better than MP2 (note that both of these methods

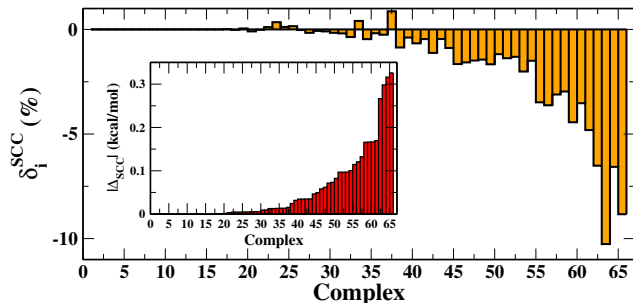


Figure 3: Difference δ_i^{SCC} of the absolute relative errors on interaction energies calculated with and without SCC for the complexes of the S66 test set (sorted with increasing $|\Delta_{\text{SCC}}|$, see inset).

have the same computational cost as the SCC-ISI-like functionals). This is quite relevant, considering that ISI-like functionals have not been explicitly constructed to model interaction energies and do not employ any empirical parameter (in contrast e.g. to the approaches in the last three lines of Table 1). Notice also that, for AC-based functionals, not only is the mean absolute error low but also the variance (last column of Tab. 1). Therefore, these functionals can describe different types of interactions with similar accuracy.

We have shown that exchange-correlation functionals built by approximating the adiabatic connection integrand with functions in which the input ingredients enter in a non-linear way can be made size-consistent at no extra computational cost. The starting idea is that size-consistency is restored once we consider fragments that are infinitely far apart, whose energy, by virtue of eq 11, we compute from the sum of quantities of individual fragments. We focused here only on the case of non-covalent interactions, but the method is generally applicable also to covalent systems. We also remark that, even though in this work we only consider a few ACMs functionals, the SCC based on eq 11 has a more general applicability to any functional built using the adiabatic connection framework as well as to any functional depending non-linearly on size-consistent global quantities.

We have shown that our SCC provides in many cases an important correction to the in-

Table 1: Mean absolute error (and variance, last column), in kcal/mol, for the S66 data set and some of its subsets, for different AC-based functionals including SCC and evaluated on Hartree-Fock density an orbitals. For all results see Table S2 in the Supporting Information. The last four lines report, for comparison, results from literature.^{55,56}

method	H-bonds	dispersion	mixed	total	variance
rev-ISI	0.35	0.44	0.20	0.33	0.08
ISI	0.37	0.42	0.19	0.33	0.09
SPL	0.42	0.42	0.19	0.35	0.11
LB	0.36	0.41	0.19	0.31	0.14
MP2	0.11	0.81	0.45	0.45	0.29
SCS-MI-MP2	0.19	0.45	0.20	0.19	0.10
SCS-CCSD	0.30	0.08	0.08	0.27	0.05
B2PLYP	0.72	2.79	1.63	1.71	1.26

teraction energy and leads to a considerable improvement of the accuracy of various ACs. Thus, it is a simple and efficient way to correct one of the main drawbacks of actual ACs, which can now be reliably used for different applications. This opens the quest for the development of improved ACs. A promising route in this direction is the construction of approximations by interpolating energy densities along the adiabatic connection, which requires non-local functionals for the strong-interaction limit^{35,57} and/or for the $\lambda = 1$ case.⁵⁸

The Supporting Information is available free of charge on the ACS Publications website at DOI:.

Acknowledgement This work was supported by the Netherlands Organization for Scientific Research (NWO) through an ECHO grant (717.013.004) and the European Research Council under H2020/ERC Consolidator Grant corr-DFT (Grant No. 648932).

Supporting Information

Mathematical forms of the used interpolation models

In this section we give mathematical forms of the used interpolation models for the AC integrand.
Interaction-Strength Interpolation (ISI):^{48,54}

$$W_\lambda^{\text{ISI}} = W_\infty[\rho] + \frac{X[\rho]}{\sqrt{1 + Y[\rho]\lambda + Z[\rho]}}, \quad (16)$$

where X , Y and Z are given by:

$$X = \frac{xy^2}{z^2}, \quad Y = \frac{x^2y^2}{z^4}, \quad Z = \frac{xy^2}{z^3} - 1 \quad (17)$$

with $x = -2W'_0[\rho]$, $y = W'_\infty[\rho]$, and $z = W_0[\rho] - W_\infty[\rho]$.

Revised Interaction-Strength Interpolation (rev-ISI):²⁸

$$W_\lambda^{\text{rISI}} = \frac{\partial}{\partial \lambda} \left(a^{\text{rISI}}[\rho]\lambda \frac{b^{\text{rISI}}[\rho]\lambda}{\sqrt{1 + c^{\text{rISI}}[\rho]\lambda + d^{\text{rISI}}[\rho]}} \right), \quad (18)$$

with:

$$\begin{aligned} a^{\text{rISI}}[\rho] &= W_\infty[\rho] \\ b^{\text{rISI}}[\rho] &= -\frac{4W'_0[\rho]W'_\infty[\rho]^2}{(W_0[\rho] - W_\infty[\rho])^2} \\ c^{\text{rISI}}[\rho] &= -\frac{8W'_0[\rho]^2W'_\infty[\rho]^2}{(W_0[\rho] - W_\infty[\rho])^4} \\ d^{\text{rISI}}[\rho] &= -1 - \frac{4W'_0[\rho]W'_\infty[\rho]^2}{(W_0[\rho] - W_\infty[\rho])^3}.e \end{aligned} \quad (19)$$

Seidl-Perdew-Levy (SPL):^{23,26,45}

$$W_\lambda^{\text{SPL}} = a^{\text{SPL}}[\rho] + \frac{b^{\text{SPL}}[\rho]}{\sqrt{1 + c^{\text{SPL}}[\rho]\lambda}} \quad (20)$$

with:

$$\begin{aligned} a^{\text{SPL}}[\rho] &= W_\infty[\rho] \\ b^{\text{SPL}}[\rho] &= W_0[\rho] - W_\infty[\rho] \\ c^{\text{SPL}}[\rho] &= -\frac{2W'_0[\rho]}{W_0[\rho] - W_\infty[\rho]}. \end{aligned} \quad (21)$$

Liu-Burke (LB):^{26,29}

$$W_\lambda^{\text{LB}} = a^{\text{LB}}[\rho] + b^{\text{LB}}[\rho] \left(\frac{1}{(1 + c^{\text{LB}}[\rho]\lambda)^2} + \frac{1}{\sqrt{1 + c^{\text{LB}}[\rho]\lambda}} \right), \quad (22)$$

with:

$$\begin{aligned} a^{\text{LB}}[\rho] &= W_\infty[\rho] \\ b^{\text{LB}}[\rho] &= \frac{W_0[\rho] - W_\infty[\rho]}{2} \\ c^{\text{LB}}[\rho] &= -\frac{4W'_0[\rho]}{5(W_0[\rho] - W_\infty[\rho])} \end{aligned} \quad (23)$$

Additional computational details

The point-charge-plus-continuum (PC) functional approximations to the strong coupling limit quantities are given by:⁵⁴

$$W_\infty[\rho] = \int \left[A\rho(\mathbf{r})^{4/3} + B \frac{|\nabla\rho(\mathbf{r})|^2}{\rho(\mathbf{r})^{4/3}} \right] d\mathbf{r} \quad (24)$$

$$W'_\infty[\rho] = \int \left[C\rho(\mathbf{r})^{3/2} + D \frac{|\nabla\rho(\mathbf{r})|^2}{\rho^{7/6}(\mathbf{r})} \right] d\mathbf{r}. \quad (25)$$

The parameters $A = -1.451$, $B = 5.317 \times 10^{-3}$, and $C = 1.535$, are determined by the electrostatic arguments⁵⁴ and $D = -2.8957 \times 10^{-2}$ has been obtained by ensuring that the given approximation to $W'_\infty[\rho]$ is exact for the helium atom.²⁸ All interaction energies reported in the letter have been corrected for the basis-set superposition error. In all calculations (except for Kr which used an aug-cc-pV5Z basis set⁵⁹) we used a basis set constructed adding selected s , p , d , and f functions to the aug-cc-pVQZ basis set^{60,61} of each element. The list of additional functions is reported in Table 2.

Results for the S66 test set

Full results for the S66 test are reported in Tables 3 and 4

References

- (1) Kohn, W.; Sham, L. J. Self-Consistent Equations Including Exchange and Correlation Effects. *Phys. Rev.* **1965**, *140*, A 1133.
- (2) Mardirossian, N.; Head-Gordon, M. Thirty years of density functional theory in computational chemistry: an overview and extensive assessment of 200 density functionals. *Mol. Phys.* **2017**, *115*, 2315–2372.
- (3) Della Sala, F.; Fabiano, E.; Constantin, L. A. Kinetic-energy-density dependent semilocal exchange-correlation functionals. *Int. J. Quantum Chem.* **2016**, *116*, 1641–1694.
- (4) Cohen, A. J.; Mori-Sánchez, P.; Yang, W. Challenges for density functional theory. *Chem. Rev.* **2012**, *112*, 289.
- (5) Burke, K. Perspective on density functional theory. *J. Chem. Phys.* **2012**, *136*, 150901.
- (6) Becke, A. D. Perspective: Fifty years of density-functional theory in chemical physics. *J. Chem. Phys.* **2014**, *140*, 18A301.
- (7) Langreth, D. C.; Perdew, J. P. *Solid State Commun.* **1975**, *17*, 1425.

Table 2: List of additional (Gaussian) basis functions used for each element.

Element	Basis function	
	type	Exponent
H	<i>s</i>	6.17937
	<i>s</i>	0.46550
	<i>p</i>	3.43000
	<i>d</i>	4.45300
He	<i>s</i>	19.0385
	<i>s</i>	2.0880
	<i>p</i>	16.1040
	<i>p</i>	2.4980
N	<i>d</i>	12.4980
	<i>s</i>	13.8234
	<i>s</i>	2.1950
	<i>p</i>	2.1480
C	<i>d</i>	6.7170
	<i>s</i>	9.9641
	<i>s</i>	1.6560
	<i>p</i>	1.5040
O	<i>d</i>	4.5420
	<i>s</i>	18.3030
	<i>s</i>	2.7760
	<i>p</i>	2.7320
Ne	<i>d</i>	8.2530
	<i>s</i>	29.0669
	<i>s</i>	4.3270
	<i>p</i>	4.2810
Ar	<i>d</i>	13.3170
	<i>s</i>	1.7580
	<i>p</i>	2.2450
	<i>d</i>	4.7760
	<i>f</i>	3.0582

Table 3: Signed errors in kcal/mol for the S66 test for all the AC-based functionals. Systems 1-23 have H-bond interaction, systems 24-46 dispersion, system 47-66 mixed characters. [Continues in Table 4]

num.	system	rev-ISI	ISI	SPL	LB
1	Water-Water	-0.064	-0.095	-0.161	-0.146
2	Water-MeOH	-0.141	-0.164	-0.213	-0.175
3	Water-MeNH2	-0.193	-0.210	-0.245	-0.189
4	Water-Peptide	-0.259	-0.294	-0.370	-0.334
5	MeOH-MeOH	-0.222	-0.239	-0.276	-0.225
6	MeOH-MeNH2	-0.364	-0.373	-0.393	-0.302
7	MeOH-Peptide	-0.417	-0.442	-0.495	-0.432
8	MeOH-Water	-0.124	-0.150	-0.204	-0.179
9	MeNH2-MeOH	-0.273	-0.287	-0.315	-0.261
10	MeNH2-MeNH2	-0.376	-0.380	-0.390	-0.293
11	MeNH2-Peptide	-0.484	-0.487	-0.494	-0.380
12	MeNH2-Water	-0.210	-0.223	-0.253	-0.180
13	Peptide-MeOH	-0.327	-0.336	-0.355	-0.272
14	Peptide-MeNH2	-0.470	-0.466	-0.460	-0.338
15	Peptide-Peptide	-0.549	-0.557	-0.575	-0.467
16	Peptide-Water	-0.156	-0.179	-0.226	-0.192
17	Uracil-Uracil	-0.649	-0.687	-0.767	-0.685
18	Water-Pyridine	-0.198	-0.209	-0.234	-0.169
19	MeOH-Pyridine	-0.296	-0.298	-0.301	-0.206
20	AcOH-AcOH	-0.481	-0.556	-0.713	-0.686
21	AcNH2-AcNH2	-0.679	-0.724	-0.819	-0.755
22	AcOH-Uracil	-0.550	-0.610	-0.739	-0.693
23	AcNH2-Uracil	-0.595	-0.647	-0.756	-0.699
24	Benzene-Benzene	0.268	0.354	0.531	0.854
25	Pyridine-Pyridine	0.350	0.448	0.652	0.998
26	Uracil-Uracil	-0.725	-0.617	-0.394	-0.002
27	Benzene-Pyridine	0.300	0.392	0.583	0.919
28	Benzene-Uracil	-0.180	-0.065	0.173	0.567
29	Pyridine-Uracil	-0.125	-0.015	0.214	0.594
30	Benzene-Ethene	0.010	0.046	0.120	0.306
31	Uracil-Ethene	-0.240	-0.205	-0.134	0.046
32	Uracil-Ethyne	-0.082	-0.056	-0.003	0.152
33	Pyridine-Ethene	0.019	0.059	0.143	0.337
34	Pentane-Pentane	-0.931	-0.913	-0.876	-0.634
35	Neopentane-Pentane	-0.671	-0.663	-0.649	-0.486
36	Neopentane-Neopentane	-0.498	-0.500	-0.502	-0.394
37	Cyclopentane-Neopentane	-0.630	-0.622	-0.605	-0.449
38	Cyclopentane-Cyclopentane	-0.736	-0.721	-0.690	-0.502
39	Benzene-Cyclopentane	-0.265	-0.215	-0.111	0.152
40	Benzene-Neopentane	-0.233	-0.202	-0.138	0.061
41	Uracil-Pentane	-0.905	-0.844	-0.718	-0.416

Table 4: [Continues from Table 3] Signed errors in kcal/mol for the S66 test for all the AC-based functionals. Systems 1-23 have H-bond interaction, systems 24-46 dispersion, system 47-66 mixed characters.

num.	system	rev-ISI	ISI	SPL	LB
42	Uracil-Cyclopentane	-0.763	-0.707	-0.591	-0.322
43	Uracil-Neopentane	-0.660	-0.625	-0.552	-0.348
44	Ethene-Pentane	-0.411	-0.409	-0.406	-0.281
45	Ethyne-Pentane	-0.148	-0.144	-0.134	-0.018
46	Peptide-Pentane	-0.902	-0.875	-0.817	-0.578
47	Benzene-Benzene	0.005	0.039	0.107	0.287
48	Pyridine-Pyridine	-0.022	0.010	0.077	0.255
49	Benzene-Pyridine	-0.002	0.029	0.093	0.268
50	Benzene-Ethyne	0.119	0.125	0.137	0.238
51	Ethyne-Ethyne	0.037	0.023	-0.005	0.021
52	Benzene-AcOH	-0.192	-0.175	-0.140	0.002
53	Benzene-AcNH2	-0.239	-0.234	-0.222	-0.106
54	Benzene-Water	-0.091	-0.094	-0.100	-0.020
55	Benzene-MeOH	-0.197	-0.177	-0.135	0.023
56	Benzene-MeNH2	-0.178	-0.155	-0.108	0.056
57	Benzene-Peptide	-0.218	-0.175	-0.086	0.141
58	Pyridine-Pyridine	-0.299	-0.299	-0.299	-0.206
59	Ethyne-Water	0.019	-0.010	-0.071	-0.071
60	Ethyne-AcOH	-0.156	-0.180	-0.229	-0.177
61	Pentane-AcOH	-0.642	-0.629	-0.603	-0.441
62	Pentane-AcNH2	-0.758	-0.742	-0.709	-0.524
63	Benzene-AcOH	-0.176	-0.141	-0.070	0.123
64	Peptide-Ethene	-0.346	-0.345	-0.344	-0.233
65	Pyridine-Ethyne	-0.040	-0.054	-0.086	-0.047
66	MeNH2-Pyridine	-0.243	-0.220	-0.173	-0.008

- (8) Gunnarsson, O.; Lundqvist, B. I. Exchange and correlation in atoms, molecules, and solids by the spin-density-functional formalism. *Phys. Rev. B* **1976**, *13*, 4274.
- (9) Colonna, F.; Savin, A. Correlation energies for some two- and four-electron systems along the adiabatic connection in density functional theory. *J. Chem. Phys.* **1999**, *110*, 2828.
- (10) Teale, A. M.; Coriani, S.; Helgaker, T. The calculation of adiabatic-connection curves from full configuration-interaction densities: Two-electron systems. *J. Chem. Phys.* **2009**, *130*, 104111.
- (11) Teale, A. M.; Coriani, S.; Helgaker, T. Accurate calculation and modeling of the adiabatic connection in density functional theory. *J. Chem. Phys.* **2010**, *132*, 164115.
- (12) Becke, A. D. A new mixing of Hartree–Fock and local density-functional theories. *J. Chem. Phys.* **1993**, *98*, 1372.
- (13) Becke, A. D. Density-functional thermochemistry. III. The role of exact exchange. *J. Chem. Phys.* **1993**, *98*, 5648.
- (14) Perdew, J. P.; Ernzerhof, M.; Burke, K. Rationale for mixing exact exchange with density functional approximations. *J. Chem. Phys.* **1996**, *105*, 9982–9985.
- (15) Grimme, S. Semiempirical hybrid density functional with perturbative second-order correlation. *J. Chem. Phys.* **2006**, *124*, 034108.
- (16) Goerigk, L.; Grimme, S. Efficient and Accurate Double-Hybrid-Meta-GGA Density Functionals Evaluation with the Extended GMTKN30 Database for General Main Group Thermochemistry, Kinetics, and Noncovalent Interactions. *J. Chem. Theory Comput.* **2010**, *7*, 291–309.
- (17) Sharkas, K.; Toulouse, J.; Savin, A. Double-hybrid density-functional theory made rigorous. *J. Chem. Phys.* **2011**, *134*, 064113.
- (18) Cramer, C. J.; Truhlar, D. G. Density functional theory for transition metals and transition metal chemistry. *Phys. Chem. Chem. Phys.* **2009**, *11*, 10757.
- (19) Fabiano, E.; Piacenza, M.; D’Agostino, S.; Sala, F. D. Towards an accurate description of the electronic properties of the biphenylthiol/gold interface: The role of exact exchange. *The Journal of Chemical Physics* **2009**, *131*, 234101.
- (20) Corminboeuf, C. Minimizing Density Functional Failures for Non-Covalent Interactions Beyond van der Waals Complexes. *Accounts of Chemical Research* **2014**, *47*, 3217–3224.
- (21) Fabiano, E.; Constantin, L. A.; Cortona, P.; Della Sala, F. Global Hybrids from the Semiclassical Atom Theory Satisfying the Local Density Linear Response. *Journal of Chemical Theory and Computation* **2015**, *11*, 122–131.
- (22) Ernzerhof, M. Construction of the adiabatic connection. *Chem. Phys. Lett.* **1996**, *263*, 499.
- (23) Seidl, M.; Perdew, J. P.; Levy, M. Strictly correlated electrons in density-functional theory. *Phys. Rev. A* **1999**, *59*, 51.
- (24) Seidl, M.; Perdew, J. P.; Kurth, S. Simulation of all-order density-functional perturbation theory, using the second order and the strong-correlation limit. *Phys. Rev. Lett.* **2000**, *84*, 5070.
- (25) Mori-Sanchez, P.; Cohen, A. J.; Yang, W. T. *J. Chem. Phys.* **2006**, *125*, 201102.

- (26) Vuckovic, S.; Irons, T. J.; Savin, A.; Teale, A. M.; Gori-Giorgi, P. Exchange–correlation functionals via local interpolation along the adiabatic connection. *J. Chem. Theory Comput.* **2016**, *12*, 2598–2610.
- (27) Cohen, A. J.; Mori-Sánchez, P.; Yang, W. Assessment and formal properties of exchange–correlation functionals constructed from the adiabatic connection. *J. Chem. Phys.* **2007**, *127*, 034101.
- (28) Gori-Giorgi, P.; Vignale, G.; Seidl, M. Electronic zero-point oscillations in the strong-interaction limit of density functional theory. *J. Chem. Theory Comput.* **2009**, *5*, 743.
- (29) Liu, Z. F.; Burke, K. Adiabatic connection in the low-density limit. *Phys. Rev. A* **2009**, *79*, 064503.
- (30) Jiang, H.; Engel, E. Orbital-dependent Representation of Correlation Energy Functional. *Zeitschrift für Physikalische Chemie* **2010**, *224*, 455–466.
- (31) Wigner, E. P. On the interaction of electrons in metals. *Phys. Rev.* **1934**, *46*, 1002.
- (32) Wigner, E. P. Effects of the electron interaction on the energy levels of electrons in metals. *Trans. Faraday Soc.* **1938**, *34*, 678.
- (33) Mirtschink, A.; Seidl, M.; Gori-Giorgi, P. Energy densities in the strong-interaction limit of density functional theory. *J. Chem. Theory Comput.* **2012**, *8*, 3097.
- (34) Zhou, Y.; Bahmann, H.; Ernzerhof, M. Construction of exchange–correlation functionals through interpolation between the non-interacting and the strong-correlation limit. *J. Chem. Phys.* **2015**, *143*, 124103.
- (35) Bahmann, H.; Zhou, Y.; Ernzerhof, M. The shell model for the exchange–correlation hole in the strong-correlation limit. *J. Chem. Phys.* **2016**, *145*, 124104.
- (36) Vuckovic, S.; Irons, T. J. P.; Wagner, L. O.; Teale, A. M.; Gori-Giorgi, P. Interpolated energy densities, correlation indicators and lower bounds from approximations to the strong coupling limit of DFT. *Phys. Chem. Chem. Phys.* **2017**, *19*, 6169–6183.
- (37) Jaramillo, J.; Scuseria, G. E.; Ernzerhof, M. Local hybrid functionals. *J. Chem. Phys.* **2003**, *118*, 1068–1073.
- (38) Maier, T. M.; Haasler, M.; Arbuznikov, A. V.; Kaupp, M. New approaches for the calibration of exchange–energy densities in local hybrid functionals. *Phys. Chem. Chem. Phys.* **2016**, *18*, 21133–21144.
- (39) Vuckovic, S.; Levy, M.; Gori-Giorgi, P. Augmented potential, energy densities, and virial relations in the weak-and strong-interaction limits of DFT. *J. Chem. Phys.* **2017**, *147*, 214107.
- (40) Arbuznikov, A. V.; Kaupp, M. Local hybrid exchange–correlation functionals based on the dimensionless density gradient. *Chem. Phys. Lett.* **2007**, *440*, 160–168.
- (41) Bahmann, H.; Kaupp, M. Efficient Self-Consistent implementation of local hybrid Functionals. *J. Chem. Theory Comput.* **2015**, *11*, 1540–1548.
- (42) Gori-Giorgi, P.; Savin, A. Degeneracy and size consistency in electronic density functional theory. *J. Phys.: Conf. Ser.* **2008**, *117*, 012017.

- (43) Savin, A. Is size-consistency possible with density functional approximations? *Chem. Phys.* **2009**, *356*, 91.
- (44) For systems with a degenerate ground-state, the presence of a system, even very far from another one, selects which degenerate ground state we should consider. In other words, each possible M^* selects a different set of degenerate states for the various A_i . The exact functional should be able to give the same ground-state energy for all the degenerate states of the fragments, something that no present XC approximation is able to do. This is interlinked with the static correlation problem in DFT.
- (45) Seidl, M.; Gori-Giorgi, P.; Savin, A. Strictly correlated electrons in density-functional theory: A general formulation with applications to spherical densities. *Phys. Rev. A* **2007**, *75*, 042511.
- (46) Liu, Z. F.; Burke, K. Adiabatic connection for strictly correlated electrons. *J. Chem. Phys.* **2009**, *131*, 124124.
- (47) Hobza, P.; Zahradnik, R. Intermolecular interactions between medium-sized systems. Nonempirical and empirical calculations of interaction energies. Successes and failures. *Chem. Rev.* **1988**, *88*, 871–897.
- (48) Fabiano, E.; Gori-Giorgi, P.; Seidl, M.; Della Sala, F. Interaction-Strength Interpolation Method for Main-Group Chemistry: Benchmarking, Limitations, and Perspectives. *J. Chem. Theory Comput* **2016**, *12*, 4885–4896.
- (49) Śmiga, S.; Fabiano, E. Approximate solution of coupled cluster equations: application to the coupled cluster doubles method and non-covalent interacting systems. *Phys. Chem. Chem. Phys.* **2017**, *19*, 30249–30260.
- (50) Ogilvie, J.; Wang, F. Y. Potential-energy functions of diatomic molecules of the noble gases: II. Unlike nuclear species. *J. Mol. Struct.* **1993**, *291*, 313–322.
- (51) Available from <http://www.turbomole.com> (accessed Nov. 2015), TURBOMOLE, V6.3; TURBOMOLE GmbH: Karlsruhe, Germany, 2011.
- (52) Furche, F.; Ahlrichs, R.; Hättig, C.; Klopper, W.; Sierka, M.; Weigend, F. Turbomole. *WIREs Comput. Mol. Sci.* **2014**, *4*, 91.
- (53) Giarrusso, S.; Gori-Giorgi, P.; Della Sala, F.; Fabiano, E. Assessment of interaction-strength interpolation formulas for gold and silver clusters. *J. Chem. Phys.* **2018**, *148*, 134106.
- (54) Seidl, M.; Perdew, J. P.; Kurth, S. Density functionals for the strong-interaction limit. *Phys. Rev. A* **2000**, *62*, 012502.
- (55) Rezáč, J.; Riley, K. E.; Hobza, P. S66: A well-balanced database of benchmark interaction energies relevant to biomolecular structures. *Journal of chemical theory and computation* **2011**, *7*, 2427–2438.
- (56) Goerigk, L.; Hansen, A.; Bauer, C.; Ehrlich, S.; Najibi, A.; Grimme, S. A look at the density functional theory zoo with the advanced GMTKN55 database for general main group thermochemistry, kinetics and noncovalent interactions. *Phys. Chem. Chem. Phys.* **2017**, *19*, 32184–32215.
- (57) Wagner, L. O.; Gori-Giorgi, P. Electron avoidance: A nonlocal radius for strong correlation. *Phys. Rev. A* **2014**, *90*, 052512.

- (58) Vuckovic, S.; Gori-Giorgi, P. Simple fully non-local density functionals for the electronic repulsion energy. *J. Phys. Chem. Lett.* **2017**, *8*, 2799–2805.
- (59) Wilson, A. K.; Woon, D. E.; Peterson, K. A.; Jr., T. H. D. Gaussian basis sets for use in correlated molecular calculations. IX. The atoms gallium through krypton. *J. Chem. Phys.* **1999**, *110*, 7667–7676.
- (60) Jr., T. H. D. Gaussian basis sets for use in correlated molecular calculations. I. The atoms boron through neon and hydrogen. *J. Chem. Phys.* **1989**, *90*, 1007–1023.
- (61) Woon, D. E.; Jr., T. H. D. Gaussian basis sets for use in correlated molecular calculations. IV. Calculation of static electrical response properties. *J. Chem. Phys.* **1994**, *100*, 2975–2988.